CERN-ACC-NOTE-2018-0015

28 February 2018
hector.garcia.morales@cern.ch

MD 2179: Scraping of off-momentum halo after injection

H.Garcia-Morales, Royal Holloway University of London, United Kingdom
R. Bruce, M. Patecki, J. Wretborn, CERN, Geneva, Switzerland

Keywords: LHC, collimation, off-momentum, halo, injection

Summary

In this MD, a beam scraping was performed using the momentum primary collimator in IR3 where dispersion is high. A second scraping was performed using a TCSG in IR7 where dispersion is almost negligible. In such a way, we aim to disentangle the contribution of off-momentum particles to halo population. These scrapings will provide useful information to better understand the usual off-momentum losses we see at the start of the ramp. The MD results would also be used to benchmark simulations of off-momentum beam losses in order to gain confidence in simulation models.

Contents

1 Introduction and motivation **2**

2 Procedure **2**

3 MD overview **2**

4 Scraping results **3**
4.1 TCP IR3 scraping 3
4.2 TCSG IR7 scraping 4

5 Disentangling the beam profiles **4**

6 Conclusions **7**

1 Introduction and motivation

This MD note summarizes the main results of the MD 2179 on "Scraping of off-momentum halo after injection". In this MD, which was carried out the 4th of November 2017, a beam scraping was performed using the momentum primary collimator in IR3 where dispersion is high. A second scraping was performed using a TCSG in IR7 where dispersion is almost negligible. In such a way, we aim to disentangle the contribution of off-momentum particles to halo population. These scrapings will provide useful information to better understand the off-momentum losses we see at the start of the ramp. The MD results would be also used to benchmark simulations of off-momentum beam losses in order to gain confidence in simulation models [1]. In Fig. 1 the BCT signal during the MD is shown. One can appreciate the different injections with their corresponding scrapings.

2 Procedure

The MD procedure can be summarized in the following steps:

1. Inject one nominal bunch.
2. Wait for 15 minutes until the bunch reaches steady state with populated off-momentum halo. This time was chosen in order to have a waiting time comparable to a typical time spent at the injection plateau in standard physics fills.
3. Scrape down with one single jaw with TCP in IR3.
4. Repeat 1, 2 and 3 but scrape with the other jaw of the TCP in IR3.
5. Repeat 1, 2, 3 and 4 but with a collimator located in a low dispersion region. In this case a horizontal TCSG (TCSG.6L7.B2) in IR7 was chosen. TCLA could not be used due to high energy deposition at this location when performing the scraping.

No additional change in the optics or the nominal collimation settings was required besides the collimator movement during the scrapings.

Table 1: Optical functions and beam sizes at the collimators used for scraping assuming gaussian distributions with $\sigma_\delta = 1.13 \cdot 10^{-4}$ and $\epsilon_n = 3.5$ μm.

Collimator	β_x [m]	D_x [m]	σ_x [mm]	σ_{xD} [mm]	σ_{xD}/σ_x
TCP.6R3.B2	131.24	-2.24	0.979	1.01	1.03
TCSG.6L7.B2	335.47	0.13	1.56	1.56	1.00

3 MD overview

The MD was carried out in B2 while B1 was used for a parallel MD. In general the MD was performed smoothly without important interruptions. In Fig. 1 the B2 BCT signal is

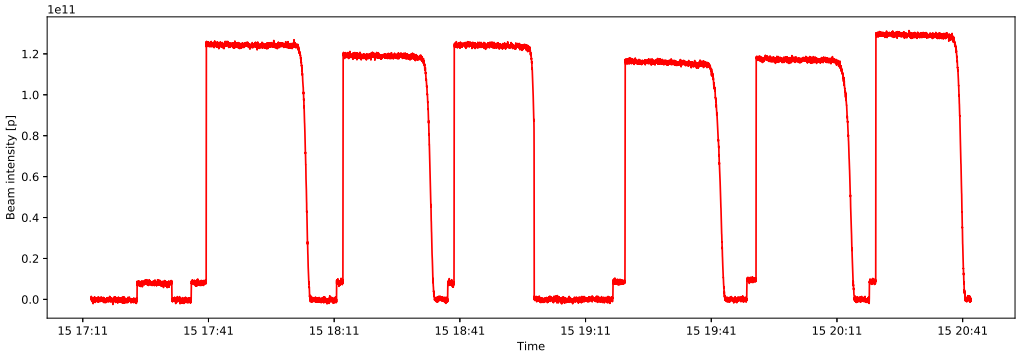

Figure 1: BCT signal in B2 during the MD. The different injections with their respective scrapings are observed.

shown as a function of the MD time. A total of six injections with its corresponding scraping were performed as they can be clearly distinguished. The procedure was followed as it is explained in previous section. We could not use the TCLA collimator as planned since high losses were observed during the scraping with a consequent beam dump. We had time to repeat the case of the scraping with right jaw in IR3 to test reproducibility.

4 Scraping results

The reconstruction of the beam profile is performed taking into account the beam losses recorded in the BLMs close to the collimator used for the scraping and the bunch intensity reduction. In Fig. 2 the BLM signal, using the 1.3 s running sum, as a function of the collimator position for each of the six scrapings is shown. The BLM signal can be translated into protons with the proper conversion factor. In this case, we have integrated the BLM signal during the scraping and we have used the intensity value at the start of the scraping to determine the total number of protons scraped. This can be seen in the right plot of Fig. 2. The noise level of the BLM signal has been subtracted and was determined by averaging the BLM signal for 60 seconds before the start of each scraping. In all case the noise level is below 10^{-6} Gy/s.

4.1 TCP IR3 scraping

The scraping was carried out using the primary collimator `TCP.6R3.B2`. The collimator position at the start of the scraping is about 8σ and the beam is fully scraped in steps of 5 μm every 2 seconds. The momentum collimator is in a high dispersion section so there are contributions from both the betatron and dispersive motion. There was some time to perform an additional scraping with the right jaw to study the reproducibility of the results. We observe that, above the noise level, the agreement of the two scrapings with the same jaw is quite good. We do not expect a perfect agreement since the beam intensity slightly varies between injections. In Fig. 3, the normalized scraped intensity as a function of the collimator position is shown for different scrapings. This is obtained by converting the BLM

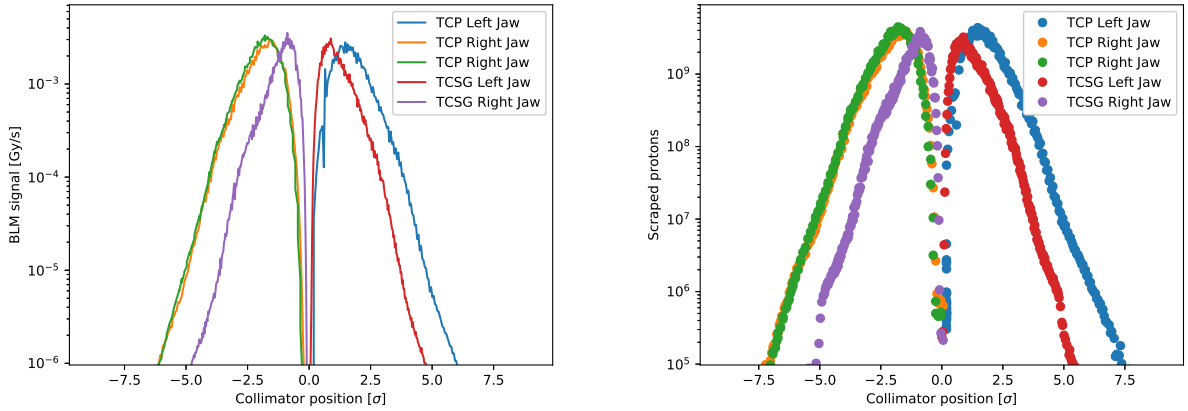

Figure 2: Left: BLM signal as a function of the collimator position. Right: Protons scraped at each collimator step, using an emittance of $\epsilon_n = 3.5$ μm

signal to protons taking into account the total scraped intensity given by the BCT for each scraping and it is normalized to the total intensity of each particular fill.

4.2 TCSG IR7 scraping

The scraping was carried out using the secondary collimator `TCSG.6L7.B2`. The collimator position at the start of the scraping is about 6σ and the beam is fully scraped in steps of 5 μm every 2 seconds. The TCSG is in a low dispersion section so the main contribution is coming from the betatron motion. As can be seen in Fig. 3, the reconstructed profile for the scrapings performed with the TCSG are narrower than those performed with the TCP in IR3 as expected.

5 Disentangling the beam profiles

Assuming that a particle horizontal position x results from the independent betatron and dispersive motions, one gets:

$$x = x_\beta + x_\delta, \tag{1}$$

where x_β is a random variable following the betatron distribution $F(x_\beta)$ and x_δ is a random variable following the dispersive distribution $F(x_\delta)$. The resulting distribution of horizontal position is therefore given by a convolution of betatron and dispersive distributions:

$$F(x) = F(x_\beta) * F(x_\delta). \tag{2}$$

A shape of the normalized scraped intensity (as shown on Fig. 3) results from folding the horizontal position distribution $F(x)$ about its maximum. If the $F(x)$ distribution is not symmetric, then what is obtained by scraping the beam with a collimator jaw is the average of the left and the right side of the distribution $F(x)$. Both betatron distribution and dispersive distribution of particles within the RF bucket are expected to be symmetric. Any

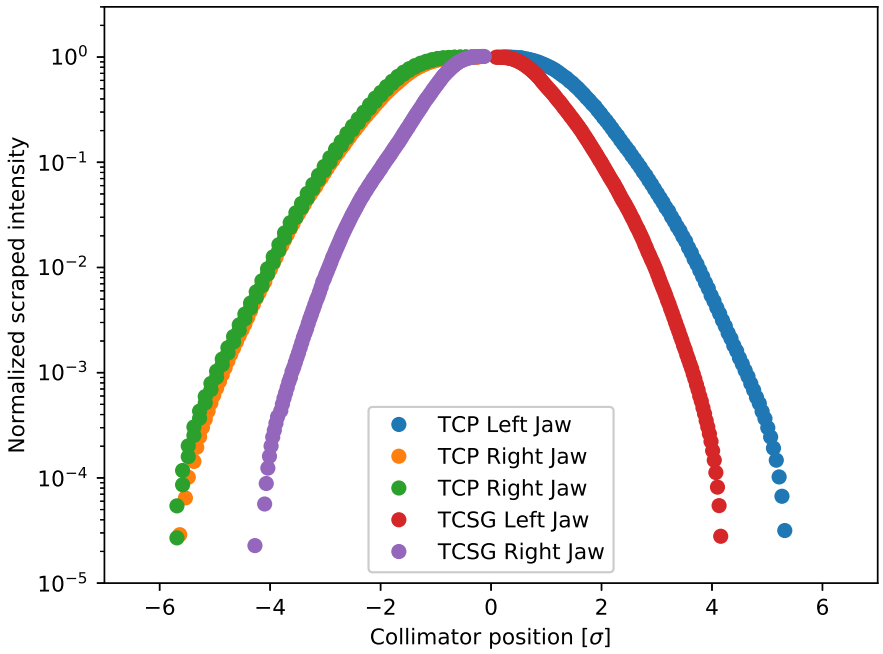

Figure 3: Normalized scraped intensity as a function of the collimator position for different scrapings for an emittance of $\epsilon_n = 3.5$ μm.

asymmetry of the $F(x)$ distribution can originate from the particles being outside of the RF bucket in the longitudinal phase-space. One can distinguish between positive and negative off-momentum values, only if the dispersive amplitude is larger than the betatron amplitude. This holds for particles outside the bucket if their betatron amplitude is smaller than $2\sigma_\beta$, so practically all particles outside the bucket. However, the negative off-momentum tail is expected to be significantly more populated comparing to the positive off-momentum tail due to dissipative effects.

The dispersive distribution $F(x_\delta)$ can be reconstructed by deconvoluting the betatron distribution $F(x_\beta)$ from the horizontal position distribution $F(x)$. We assume that $F(x)$ is represented by the normalized scraped intensity taken at IR3 and the betatron distribution $F(x_\beta)$ is represented by the normalized scraped intensity taken at IR7 where the contribution from the dispersion is small. We also assume that bunches scraped at IR3 and IR7 were identical. The applied method is based on transforming both $F(x)$ and $F(x_\beta)$ to the frequency space using the fast Fourier transform algorithm (FFT).

$$F(x) \xrightarrow[\text{FFT}]{} \hat{F}(\hat{x}), \tag{3}$$

$$F(x_\beta) \xrightarrow[\text{FFT}]{} \hat{F}(\hat{x}_\beta). \tag{4}$$

In a frequency space a convolution becomes multiplication and Eq. 2 becomes:

$$\hat{F}(x) = \hat{F}(\hat{x}_\beta)\hat{F}(\hat{x}_\delta). \tag{5}$$

The desired dispersive distribution $F(x_\delta)$ is therefore given by:

$$F(x_\delta) \xleftarrow[\text{iFFT}]{} \hat{F}(\hat{x}_\delta) = \frac{\hat{F}(\hat{x})}{\hat{F}(\hat{x}_\beta)}, \tag{6}$$

where iFFT denotes the inverse Fourier transform.

It is worth to mention that the shape of both $F(x)$ and $F(x_\beta)$ is close to a gaussian, sampled with about 100 points. After switching into the frequency domain, the number of relevant points decreases to about 10, while the rest is hidden behind the noise and fluctuates close to 0. It is therefore necessary to mask the irrelevant points (set them to 0 in $\hat{F}(x)$), otherwise the noise would be enhanced.

Such obtained $F(x_\delta)$ distribution is depicted on Fig. 4. Black stars represent the result of the deconvolution, red line is a Gaussian fit to the core and blue line is a Gaussian fit to the residual between the black stars and the red line. A spread of the core of the momentum

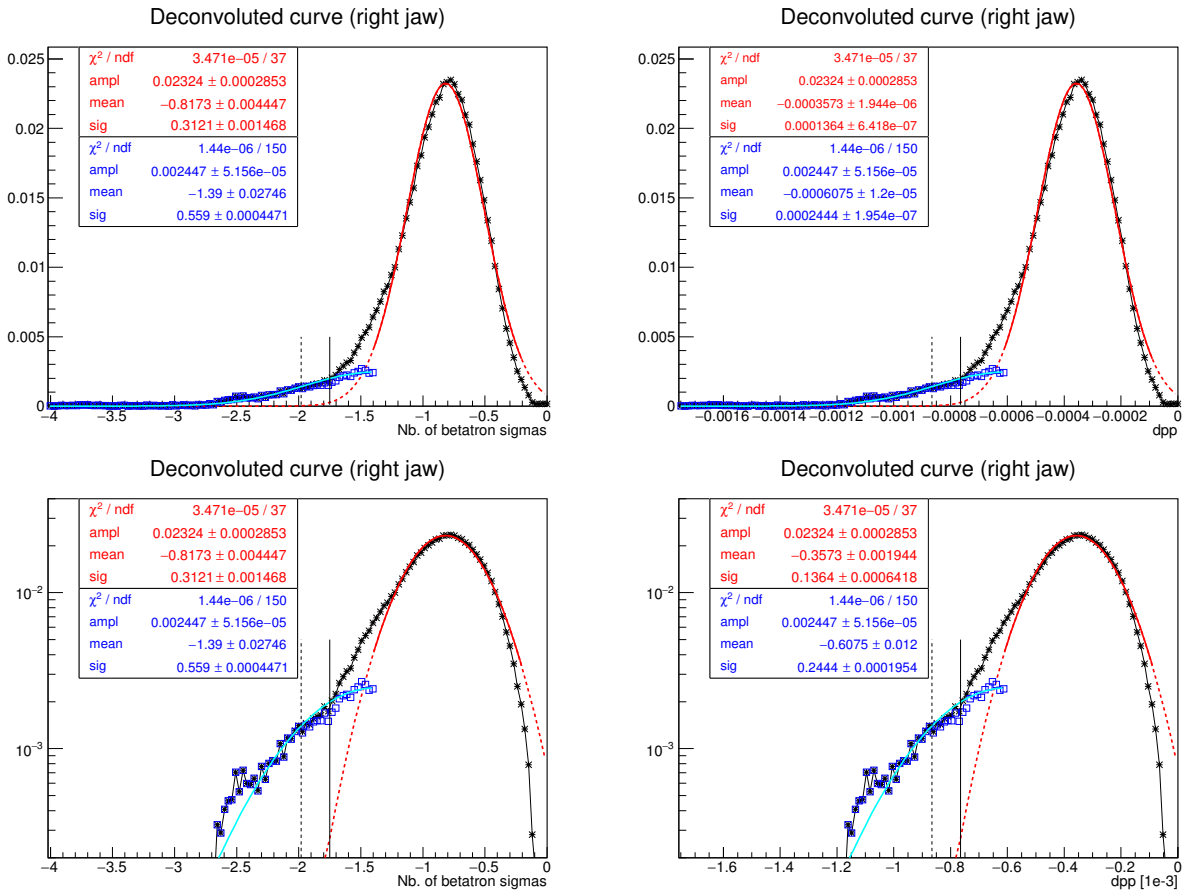

Figure 4: Top left: Dispersive distribution in a linear scale as a number of betatron beam sigma. Top right: Momentum offset distribution in a linear scale. Bottom: same as top but in a log scale.

offset distribution (red line in Fig. 4, right column) is $1.36 \cdot 10^{-4}$, close to the reference value for the LHC of $1.13 \cdot 10^{-4}$. A tail of the momentum offset distribution is well visible on

the left from the core. A dashed vertical line corresponds to the theoretical bucket height value, while a solid vertical line corresponds to a value where we notice a change in slope of the tail distribution. These two observations suggest that the blue line characterizes the particles being close to or outside of the separatrix. However, what we interpret as an off-momentum tail might be highly affected by the enhanced noise when performing the deconvolution. Better reconstruction of the off-momentum profile can be obtained when the dispersive contribution is comparable to the betatron distribution, which currently is not the case. This could be improved by increasing the dispersion at the IR3 collimator, at least a few times. Another source of error may come from the non-reproducibility of the consecutive bunches. Ideally, the measurements should be repeated several times to study the reproducibility of the results between different injections.

6 Conclusions

The MD was carried out smoothly and the goal of measuring the beam profile using collimator scrapings with two different collimators was fulfilled. We observed clear differences in the beam profile reconstruction performed in two different locations, one in a high dispersion section (IR3) and one in a low dispersion section (IR7). As expected, the profile in a high dispersion section contains an additional contribution coming from the natural energy spread of the beam. A first try to disentangle the contributions of the betatron and off-momentum halo has been presented and shows a clear tail of particles outside the RF bucket. However, for fully conclusive results, the measurements should be repeated in order to study the reproducibility.

References

[1] J. Wretborn et al., "Study of off-momentum losses at the start of the ramp in the Large Hadron Collider", CERN-ACC-NOTE-2017-0065, (2017)